

Structure Functions and Parton Distributions

Jianwei Qiu^{a*}

^aDepartment of Physics and Astronomy, Iowa State University,
Ames, Iowa 50011, U.S.A.

In this talk, I review the status of theoretical understanding of nuclear structure functions and parton distributions and discuss the constraints on nuclear parton distributions from existing data and the global QCD analysis.

1. Introduction

Much of the predictive content of perturbative QCD (pQCD) treatment of the hadronic hard scattering is contained in factorization theorems [1]. Their purpose is to separate long- from short-distance effects in scattering amplitudes. They supply perturbatively uncalculable long-distance effects with physics content in terms of well-defined matrix elements, which allows them to be measured experimentally or by numerical simulation. They also define the normalization of short-distance factors, which allows them to be calculated perturbatively. Predictions follow when processes with different hard scatterings but the same nonperturbative matrix elements are compared. Thus, quark and gluon distributions measured in deep inelastic scattering may be used to normalize the Drell-Yan or jet cross section.

Deep inelastic lepton scattering has long been regarded as the cleanest probe of constituent substructure. Considerable interest, therefore, greeted the observation [2] by European Muon Collaboration (EMC) that the structure function $F_2(x_B, Q^2)$ of an iron nucleus differs in significant ways as a function of x_B from that for deuterium. It was the discovery of the EMC effect that opened a door for systematic study of QCD dynamics in a nuclear environment, which has led to many new QCD phenomena, e.g., shadowing, saturation, and color glass condensate.

In this talk, I review our abilities and limitations to generalize the pQCD factorization theorems to the hard scattering involving nuclei. Nuclear parton distributions are heavily used in phenomenological description of hard processes in heavy ion reactions at SPS and RHIC energies and in calculating predictions at the LHC energies. According to the factorization theorems, nuclear dependence of parton distributions should be universal or process independent. I discuss the constraints on nuclear parton distributions from existing data and the global QCD analysis.

*jwq@iastate.edu. I thank Eskola and Salgado for useful discussions and figures. This work is supported in part by the United States Department of Energy under Grant No. DE-FG02-87ER40371.

2. Structure Functions and Parton Distributions

2.1. Structure functions

An inclusive deep inelastic scattering (DIS) process is generically of the form, $\ell(E) + h(p) \implies \ell(E') + X$, where ℓ represents a lepton, h a hadron (a nucleon or nucleus), and X an arbitrary hadronic final-state. The process, illustrated in Fig. 1(a), is initiated by the exchange of a virtual photon (or a vector boson in general). In DIS, the momentum transfer between the lepton and the hadron, q , is spacelike, $-q^2 = Q^2$. The Bjorken scaling variable is defined as $x_B = \frac{Q^2}{2p \cdot q} = \frac{Q^2}{2m_h \nu}$, where ν is the energy transferred from the lepton to the hadron in the hadron (target) rest frame, $\nu = E - E'$. In the same frame, $Q^2 = 4EE' \sin^2(\theta/2)$ with the lepton scattering angle θ .

≈0.8cm

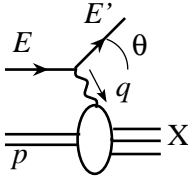


Figure 1(a)

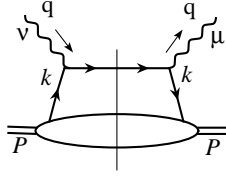


Figure 1(b)

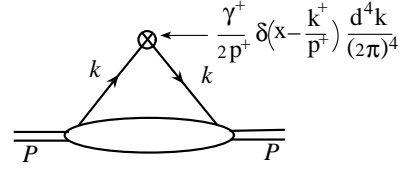


Figure 2

≈0.7cm

The DIS cross section with unpolarized beam and target can be written in the one photon exchange approximation as [3]

$$\frac{d\sigma^{\text{DIS}}}{dx_B dQ^2} = \frac{\sigma_{\text{Mott}}}{EE'} \frac{\pi F_2(x_B, Q^2)}{\epsilon x_B} \left[\frac{1 + \epsilon R(x_B, Q^2)}{1 + R(x_B, Q^2)} \right], \quad (1)$$

where ϵ is a kinematic parameter and R is the ratio of longitudinal to transverse photon-hadron cross section, $R = \sigma_L/\sigma_T = [(1 + 4x_B^2 m^2/Q^2) F_2 - 2x_B F_1]/[2x_B F_1]$. The functions F_1 and F_2 are called *structure functions* and defined as

$$F_i(x_B, Q^2) \equiv e_i^{\mu\nu} W_{\mu\nu}(x_B, Q^2) \quad (2)$$

with $i = 1, 2$ and projection tensors $e_i^{\mu\nu}$ given in Ref. [3]. The $W_{\mu\nu}(x_B, Q^2)$ is the DIS hadronic tensor and is proportional to the square of the hadronic part in Fig. 1(a) or the imaginary part of the forward scattering amplitude in Fig. 1(b). The structure functions F_1 and F_2 contain all complex hadronic interactions of the DIS cross section.

The structure functions are *locally* defined in DIS and can be directly extracted from measured DIS cross section via Eq. (1). Because DIS cross section depends on both hard scattering scale Q^2 and soft momentum scale intrinsic to hadron wave function $1/\text{fm} \sim \Lambda_{\text{QCD}}$, structure functions F_1 and F_2 are nonperturbative quantities.

2.2. Parton distribution functions

Parton distributions (or parton distribution functions), $\phi_{f/h}(x, \mu^2)$, are defined as matrix elements of a pair of parton fields and are often interpreted as the probability densities

for finding a parton of flavor f within a hadron h of momentum p , with its momentum fraction between x and $x + dx$ and its virtuality less than μ^2 [4]. For example, a quark distribution is given by

$$\phi_{q/h}(x, \mu^2) = \int \frac{dy^-}{2\pi} e^{ixp^+y^-} \langle h(p) | \bar{\psi}_q(0) \frac{\gamma^+}{2} \mathcal{P} e^{-ig \int_0^{y^-} dw^- A^+(w^-)} \psi_q(y^-) | h(p) \rangle . \quad (3)$$

Corresponding Feynman diagrams in momentum space are given by the type of cut-vertex diagrams in Fig. 2 [5].

Parton distributions are *universally* defined and in principle, independent of any specific physical process. Because of the hadron state, like the structure functions, parton distributions are nonperturbative quantities. However, unlike the structure functions, parton distributions are not *direct* physical observables.

≈0.8cm

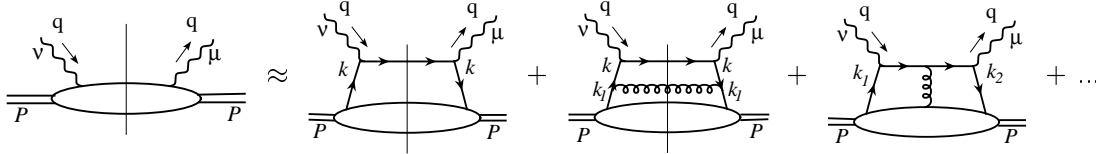


Figure 3

≈1.3cm

2.3. Factorization

Structure functions and parton distributions are related to each other via perturbative QCD factorization [6].

In QCD perturbation theory, the forward scattering amplitude in Fig. 1(b) can be represented in terms of an expansion of Feynman diagrams illustrated in Fig. 3. However, because of the soft momentum scale in the hadron state, Feynman diagrams in Fig. 3 are not entirely calculable in perturbation theory. For example, the integration of loop momentum k for the leading order (LO) diagram can be expressed as

≈0.8cm

$$\int d^4k \left(\text{quark-gluon vertex} \right) \left(\text{hadron state} \right) \Rightarrow \int d^4k H(Q, k) \left(\frac{i}{k^2 + i\epsilon} \right) \left(\frac{i}{k^2 - i\epsilon} \right) T(k, p)$$

≈0.8cm

which is completely dominated by the phase space near $k^2 \sim (1/\text{fm})^2 \sim \Lambda_{\text{QCD}}^2$ because of the perturbative pinch singularity at $k^2 \sim 0$. Therefore, when $k^2 \ll Q^2$, the dominant contribution to the DIS cross section comes from the phase space where the active quark is “long-lived” relative to the time scale of hard collision, $t_c \sim 1/Q$. It is such a “long-lived” parton state that separates long- from short-distance effects in the cross section.

≈0.75cm

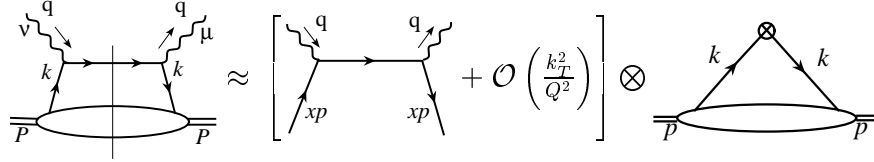


Figure 4

≈0.8cm

In terms of a power expansion of $\langle k^2 \rangle / Q^2$, the LO forward scattering amplitude in Fig. 3 can be approximated as illustrated in Fig. 4, and corresponding contribution to structure function F_2 can be expressed as

$$F_2(x_B, Q^2) = x_B \sum_q e_q^2 \phi_{q/h}(x_B) + \mathcal{O}\left(\frac{\Lambda_{\text{QCD}}^2}{Q^2}\right). \quad (4)$$

If we neglect *all* high order diagrams and power corrections in $1/Q^2$, F_2 in Eq. (4) has the Bjorken scaling in x_B and is the same as the prediction of the parton model.

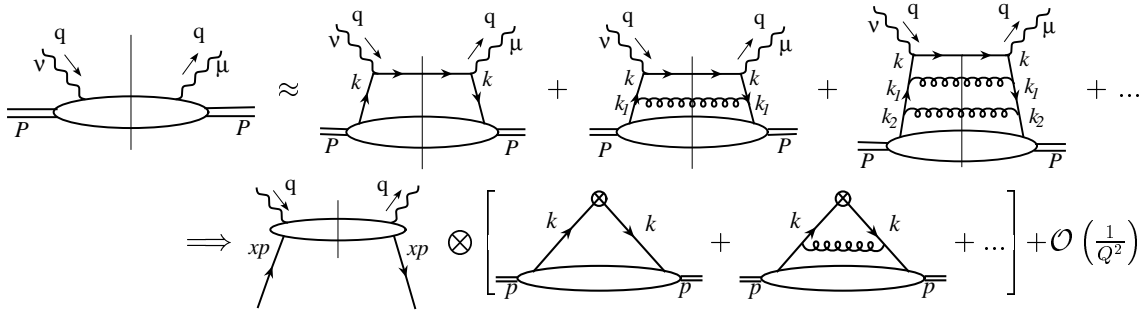


Figure 5

≈0.8cm

However, QCD is much richer in dynamics than Feynman's parton model, and the rest diagrams in Fig. 3 will all contribute to the measured structure functions. Although there are infinite diagrams, leading contributions to $W_{\mu\nu}$ in a physical gauge come from the diagrams with a ladder structure, as illustrated in Fig. 5, and partons' loop momentum integrations $\int d^4 k_i$ are dominated by the region of phase space near the perturbative pinch singularities, $k_i^2 \sim 0$. By neglecting the power corrections of $\langle k_i^2 \rangle / Q^2$, as illustrated in Fig. 5, the sum of all ladder diagrams in Fig. 5 can be factorized into a convolution of a short-distance part with all momentum scales of the order of Q^2 and a long-distance nonperturbative parton distribution [6],

$$F_2(x_B, Q^2) = \sum_f \int_{x_B}^1 \frac{dx}{x} C_f \left(\frac{x_B}{x}, \frac{Q^2}{\mu^2}, \alpha_s(\mu) \right) \phi_{f/h}(x, \mu^2) + \mathcal{O}\left(\frac{\Lambda_{\text{QCD}}^2}{Q^2}\right) \quad (5)$$

where \sum_f runs over all parton flavors, the coefficient functions C_f are perturbatively calculable in a power series of α_s , and the parton distributions $\phi_{f/h}$ represent the leading

and universal part of the long-distance physics. All other nonperturbative contributions are powerfully suppressed.

If the scattering is hard enough for neglecting all power corrections, Eq. (5) represents a fact that parton distributions, though theoretically defined, can be experimentally measured via the physical quantities like the structure functions. It also indicates that a test of QCD in high energy collisions requires a good knowledge of parton distributions.

2.4. Global analyses of parton distributions

Although parton distributions are nonperturbative, their dependence on the factorization scale μ^2 is predicted by pQCD in a form of DGLAP evolution equations [7],

$$\mu^2 \frac{\partial}{\partial \mu^2} \phi_{i/h}(x, \mu^2) = \sum_j \int_x^1 \frac{dx'}{x'} P_{i/j} \left(\frac{x}{x'}, \alpha_s(\mu) \right) \phi_{j/h}(x', \mu^2) \quad (6)$$

with calculable splitting functions $P_{i/j}$ for $\mu^2 \gg \Lambda_{\text{QCD}}^2$. To solve for the parton distributions, we need a set of input parton distributions at μ_0^2 , which can only be extracted from experimental data.

The global QCD analysis of parton distributions represents our effort to find a best set of universal parton distributions from all existing data. The analysis itself is an excellent test of QCD dynamics in the hard scattering, the factorization theorems, and the universality of parton distributions. With the extracted parton distributions of a free nucleon, pQCD calculations with next-to-leading order (NLO) accuracy in α_s are consistent with thousands of data points from more than dozen physical observables in hadronic collisions [8, 9]. Since the factorization theorems determine the absolute normalization for each observable, there is no need for any artificial K -factor.

3. Nuclear Structure Functions and Parton Distributions

3.1. Definitions

The derivation of the DIS cross section in Eq. (1) is independent of the details of the targets. Nuclear structure functions, $F_i^A(x_B, Q^2)$, extracted from DIS data on a nuclear target of atomic weight A , are defined in the same way as that in Eq. (2) with the hadronic tensor of a nuclear state. The Bjorken variable, $x_B \equiv \frac{Q^2}{2p \cdot q}$ with an averaged nucleon momentum $p = \frac{P_A}{A}$, and has a range from 1 to A .

If the partons' typical virtuality in a nucleus, $\langle k^2 \rangle_A \ll Q^2$, and $\langle k_T \rangle_A \ll xp$, all derivations in last section for a free nucleon state can be carried over for a nuclear state, and nuclear structure function, F_2^A , shares the same factorized relation,

$$F_2^A(x_B, Q^2) = \sum_f \int_{x_B}^1 \frac{dx}{x} C_f \left(\frac{x_B}{x}, \frac{Q^2}{\mu^2}, \alpha_s(\mu) \right) \phi_{f/A}(x, \mu^2) + \mathcal{O} \left(\frac{\langle k^2 \rangle_A}{Q^2} \right) \quad (7)$$

where the short-distance coefficient functions C_f should be the same as those for free nucleon and independent of A . In Eq. (7), nuclear parton distributions, $\phi_{f/A}(x, \mu^2)$, are matrix elements of nuclear states with the same operators of nucleon parton distributions.

If we can neglect the power corrections in Eq. (7), i.e., pQCD factorization theorems hold, we can extract nuclear parton distributions and their A -dependence from the measured structure functions on nuclear targets. Because of the universality of parton dis-

tributions, the extracted A -dependence of nuclear parton distributions should also be universal and represent the internal properties of a nuclear wave function.

≈0.7cm

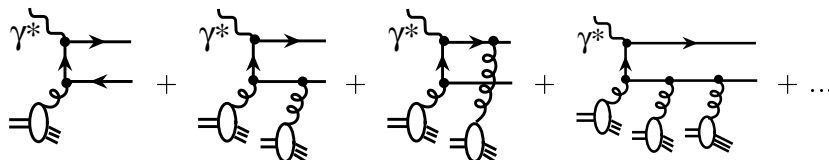


Figure 6

≈1.0cm

3.2. Nuclear shadowing

Gluon distribution grows rapidly as momentum fraction x decreases. When $x_B \ll 0.1$, a nucleus becomes a dense system of small- x gluons and the large number of soft gluons from different nucleons can all participate in the hard scattering, as illustrated in Fig. 6. Such coherent multi-gluon interactions suppress nuclear structure function $F_2^A(x_B, Q^2)$ in comparison to a sum of free nucleon structure functions. Such suppression is often referred as nuclear shadowing, and it increases as x_B decreases and/or A increases.

$$F_2^g(x_B, Q^2) \propto \left[\begin{array}{c} \gamma^* \quad \gamma^* \\ \leftarrow k \quad \rightarrow k \\ \text{---} \text{---} \text{---} \text{---} \\ \text{---} \text{---} \end{array} + \begin{array}{c} \gamma^* \quad \gamma^* \\ \leftarrow k \quad \rightarrow k \\ \text{---} \text{---} \text{---} \text{---} \\ \text{---} \text{---} \text{---} \text{---} \end{array} + \dots \right]$$

$$\Rightarrow \begin{array}{c} q \quad q \\ \leftarrow \quad \rightarrow \\ \text{---} \text{---} \\ \text{---} \text{---} \end{array} \otimes \left[\begin{array}{c} k \quad k \\ \text{---} \text{---} \text{---} \text{---} \\ \text{---} \text{---} \end{array} + \begin{array}{c} k \quad k \\ \text{---} \text{---} \text{---} \text{---} \\ \text{---} \text{---} \text{---} \text{---} \end{array} + \dots \right] + \mathcal{O}\left(\frac{1}{Q^2}\right)$$

Figure 7

≈0.8cm

In order to understand the phenomenon of nuclear shadowing in a language close to pQCD factorization, let's consider a leading twist (or leading power) gluonic contribution to the structure function F_2 , as illustrated in Fig. 7. If the active quark's virtuality in a large nucleus, $\langle k^2 \rangle_A \ll Q^2$, the multiple gluonic contributions are dominated by the phase space where the quark state is "long-lived", which separates long- from short-distance effects, and pQCD factorization holds. Unlike what shown in Fig. 5, nuclear quark distribution in Fig. 7 gets contributions from multi-gluon interactions from different nucleons. Since $\langle k^2 \rangle_A \ll Q^2$, such multi-gluon interactions are remote from the short distance hard scattering, and thus, are internal to nuclear parton distributions.

If the factorization scale μ^2 is within perturbative region, multi-gluon interactions in Fig.7 lead to calculable corrections to DGLAP equations. The first corrections, in the

in Fig. 6, are equally important. If the intrinsic parton virtuality in such a dense system, $\langle k^2 \rangle_A \sim Q_s^2 \gg \Lambda_{\text{QCD}}^2$, the active partons are “short-lived”, and multiple gluonic contributions to the structure functions in Fig. 6 or 7 might be calculated without introducing a “sea” quark distribution. The calculation can be carried out in the target rest frame as illustrated in Fig. 8, and the saturated nuclear structure function F_2^A is given by [12]

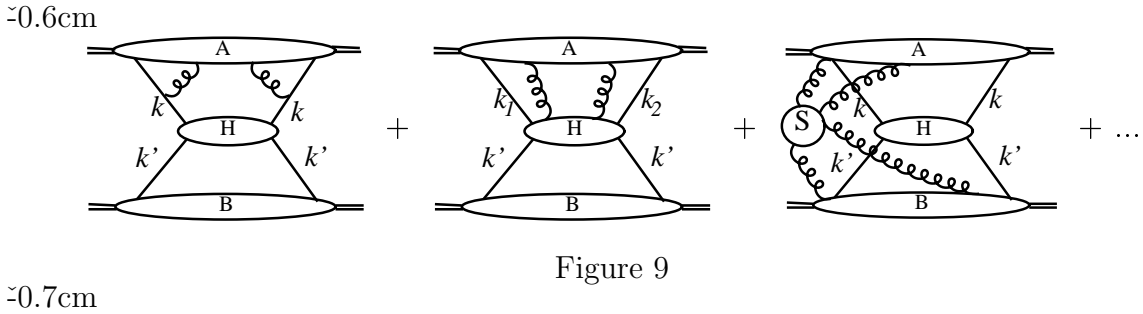
$$F_2^A \propto \int d^2b dz \left| \psi_{\gamma^* \rightarrow q\bar{q}}(b, z, Q^2) \right|^2 \sigma_{q\bar{q}-A}(b, z, Q_s^2) \quad (9)$$

where $\psi_{\gamma^* \rightarrow q\bar{q}}$ is the wavefunction for a virtual photon to go into a quark-antiquark pair of longitudinal momentum fractions z and $1 - z$, b is a Fourier conjugate of relative momentum between q and \bar{q} , and $\sigma_{q\bar{q}-A}$ represents a hadronic cross section between the $q\bar{q}$ pair and the nucleus.

In this saturation regime, the pQCD factorization formula in Eq. (7) is not valid. What calculated in this saturation limit are nuclear structure functions including all power corrections, not the parton distributions, which, by definition, are twist-2 matrix elements and universal.

3.4. Factorization in heavy ion collisions

For a hard probe of scale Q in relativistic heavy ion collisions, there could be three types of multi-gluon interactions: (1) within individual ion, (2) between the hard scattering and one or both ions, and (3) between two ions, as illustrated in Fig. 9.



If the parton virtuality $k^2 \ll Q^2$, the first type soft gluon interactions are remote from the hard probe and internal to individual ion, and therefore, should have been included in nuclear parton distributions and do not interfere with pQCD factorization. The second type of multi-gluon interactions with physical polarizations are suppressed by powers of $\langle k^2 \rangle / Q^2$ because they link effects at two different scales. If soft gluon interactions with the hard part involve only one ion, a generalized factorization for leading power corrections should be valid for calculating this type of interactions [13].

The third type of multi-gluon interactions is the most difficult one to remove. Such soft gluon interactions exchange informations between two ions, and therefore, have a potential to alter the parton distributions before the hard scattering takes place. Without the universality of parton distributions, pQCD calculations do not have real predictive power. Due to the gauge invariance of QCD and unitarity, contributions of the third type soft gluon interactions to a physical observable are suppressed by a power of $(1/Q^4)$ [13].

Therefore, pQCD factorization formalism for hadronic collisions can apply to hard probes in heavy ion collisions so long as the power corrections are relatively small,

$$\frac{d\sigma_{AB}}{dQ^2} = \sum_{a,b} \phi_{a/A}(x_a, \mu^2) \otimes \phi_{b/B}(x_b, \mu^2) \otimes H_{ab} \left(x_a x_b S, \frac{Q^2}{\mu^2}, \alpha_s(\mu) \right) + \mathcal{O} \left(\frac{\langle k^2 \rangle}{Q^2} \right) \quad (10)$$

where \otimes represents convolution over parton momentum fractions x_a and x_b . One can also include nuclear thickness functions into Eq. (10) to take care of the size effect of the ions. At this leading power level, A -dependence of an observable is completely determined by nuclear parton distributions.

When the hard scale $Q \ll S$, momentum fractions of the active partons can be very small. Soft gluon interactions between two ions, in addition to the interactions within individual ion, can lead to a much larger Q_s^2 in heavy ion collisions than that in DIS. When Q is not too much larger than Q_s , pQCD factorization fails, and normal concept of parton distributions cannot be applied to such a dense system.

If the power corrections are significant, but not too large, pQCD calculations might be systematically carried out at the first power corrections. The predictions are often expressed in terms of multi-parton correlation functions [14].

4. Global Analysis of Nuclear Parton Distribution Functions

4.1. Methodology

Predictive power of pQCD calculations of hard probes in heavy ion collisions relies on a set of universal nuclear parton distributions. Therefore, a reliable set of nuclear parton distributions is crucial for understanding RHIC physics. Any new physics and phenomena should represent the observations beyond what predicted by pQCD factorization.

PQCD predicts the scale dependence of parton distributions in terms of evolution equations. Before performing a global QCD analysis of nuclear parton distributions, we are required to choose: (1) evolution equations, (2) parameterizations of input nuclear parton distributions at a scale μ_0^2 , and (3) data sets with rich nuclear information. Then, we need to (1) evolve the input distributions to any other values of μ^2 , (2) calculate the theoretical predictions by using the evolved distributions, and (3) compare the predictions with real data and calculate the χ^2 . The best set of nuclear parton distributions should give a minimum χ^2 or a best fit to all existing data.

At the leading twist level, A -dependence of all physical observables are completely determined by the nuclear dependence of the parton distributions. Deriving a reliable A -dependence of parton distributions is a most crucial part of the global analysis. There are two possible approaches to derive the A -dependence: (A) DGLAP evolution with all A -dependence included in the input distributions at μ_0^2 and (B) modified evolution equations of the type in Eq. (8) with nonperturbative A -dependence included in the input distributions at μ_0^2 and perturbative A -dependence generated from the evolution.

4.2. Existing work

Two groups have been doing global analysis of nuclear parton distributions. Eskola, Kolhinen, Ruuskanen, and Salgado (EKRS) produced EKS98 package of nuclear parton distributions [15]. Hirai, Kumano, and Miyama (HKM) derived several sets of nuclear parton distributions from extensive DIS data [16].

Both groups used LO DGLAP evolution equations and adopted the approach (A) for including nuclear dependence. They define the input parton distributions as

$$\phi_{f/A}(x, \mu_0^2) = R_f^A(x, \mu_0^2) \phi_{f/N}(x, \mu_0^2) \quad (11)$$

with $\phi_{f/N}(x, \mu_0^2)$ are known free nucleon parton distributions. EKRS used both CTEQ-LO and GRV-LO free nucleon parton distributions for producing EKS98, while HKM used MRST-LO parton distribution for its nuclear parton distributions. Two groups used different parameterizations for $R_f^A(x, \mu_0^2)$. The goal of the global analysis is to extract the ratio $R_f^A(x, \mu_0^2)$ that represents a best fit to all data used in the analysis.

For data selection, two groups used different data sets to produce their published nuclear parton distributions [15, 16]. EKRS used both DIS and Drell-Yan data on nuclear targets. In particular, Drell-Yan data from Fermilab E772 experiment help to fix relative nuclear effects in valence and sea and make the ratio for sea quarks, $R_S(x, \mu_0^2) < 1$ at medium x . In addition, EKRS used NMC data on Q^2 -dependence of $F_2^{\text{Sn}}/F_2^{\text{C}}$ that provide constraints on $R_g^A(x, \mu_0^2)$. On the other hand, HKM used only DIS data.

Detailed comparison between data and theoretical calculations using EKRS nuclear parton distributions and other available parameterizations can be found in Ref. [17]. Similar comparison for HKM distributions can be found in Refs. [16, 17]. Both published EKRS and HKM nuclear parton distributions can fit their selected data sets very well. I summarize a few key differences here: (1) there are large differences in input distributions at $\mu_0^2 = 2.25 \text{ GeV}^2$; (2) the default set of nuclear parton distributions in HIJING seems to give a too strong A -dependence; and (3) HKM distributions appear to predict a different Q^2 -dependence for NMC data on the ratio $F_2^{\text{Sn}}/F_2^{\text{C}}$ and a different shape in x_2 dependence for E772 Drell-Yan data.

Notice that both of these data were not included in the HKM's original global analysis. Since DIS data are only sensitive to the sum of quark and antiquark distributions, it should not be surprised that the separation of sea and valence quarks in HKM distributions is not very well constrained. Because LO structure function F_2 does not have an explicit dependence on gluon distribution, gluons could not be well constrained by DIS data alone. These two ambiguities are reduced in EKRS approach because of the usage of Drell-Yan data and NMC data on Q^2 -dependence of $F_2^{\text{Sn}}/F_2^{\text{C}}$.

5. Summary and Outlook

Much of the predictive power of pQCD calculations relies on the factorization and universality of parton distributions. PQCD calculations with next-to-leading order accuracy in α_s have been consistent with almost all existing data from hadronic collisions without a need for an artificial K -factor.

PQCD factorization theorems can be applied to hard scattering involving nuclei, if the partonic system covered by the interaction volume is a dilute system, in which partons are “free” or “long-lived” at the time scale of hard collision. If the leading twist pQCD factorization theorems hold, A -dependence of all observables are completely determined by the universal A -dependence of nuclear parton distributions. Any significant deviation from the predicted A -dependence is a signal of breakdown of the conventional pQCD factorization and new physical phenomena. Therefore, precise A -dependence of nuclear

parton distributions are very important for understanding hard scattering signals in heavy ion collisions at RHIC and the LHC energies.

Nuclear dependence of the input distributions is a main source of the A -dependence of nuclear parton distributions and has to be extracted from better data. At high energy or small- x , perturbative A -dependence via the modified evolution equations might be important too. Two sets of nuclear parton distributions from LO global QCD analysis are available. In order to reach the same level of precision tests that achieved in collisions with free hadrons, we need NLO nuclear parton distributions with better precisions on the A -dependence.

REFERENCES

1. J. C. Collins, D. E. Soper and G. Sterman, *in* Perturbative Quantum Chromodynamics, ed. A.H. Mueller, Adv. Ser. Direct. High Energy Phys. **5**, 1 (1988).
2. J. Ashman et al. (EM Collaboration), Phys. Lett. **B123**, 275 (1983).
3. X. f. Guo, J. w. Qiu and W. Zhu, Phys. Lett. B **523**, 88 (2001).
4. J. C. Collins and D. E. Soper, Nucl. Phys. B **194**, 445 (1982).
5. A. H. Mueller, Phys. Rept. **73**, 237 (1981).
6. G. Curci, W. Furmanski and R. Petronzio, Nucl. Phys. B **175**, 27 (1980).
7. Yu. Dokshitzer, Sov. Phys. JETP **46**, 1649 (1977); V.N. Gribov and L. N. Lipatov, Sov. Nucl. Phys. **15**, 438, 675 (1972); G. Altarelli, G. Parisi, Nucl. Phys. B **126**, 298 (1977).
8. A. D. Martin, R. G. Roberts, W. J. Stirling and R. S. Thorne, Eur. Phys. J. C **23**, 73 (2002); Phys. Lett. B **531**, 216 (2002).
9. J. Pumplin *et al.* JHEP **0207**, 012 (2002).
10. A. H. Mueller and J. w. Qiu, Nucl. Phys. B **268**, 427 (1986).
11. J. w. Qiu, Nucl. Phys. B **291**, 746 (1987).
12. A.H. Mueller (Plenary talk at this conference), and references therein.
13. J. w. Qiu and G. Sterman, Nucl. Phys. B **353**, 137 (1991).
14. J. w. Qiu and G. Sterman, arXiv:hep-ph/0111002.
15. K. J. Eskola, V. J. Kolhinen and P. V. Ruuskanen, Nucl. Phys. B **535**, 351 (1998); K. J. Eskola, V. J. Kolhinen and C. A. Salgado, Eur. Phys. J. C **9**, 61 (1999).
16. M. Hirai *et al.*, Phys. Rev. D **64**, 034003 (2001); nuclear parton distributions are available at the <http://hs.phys.saga-u.ac.jp/nuclp.html>.
17. K.J. Eskola *et al.*, arXiv:hep-ph/0110348; arXiv:hep-ph/0205231.